Excitonic clusters in coupled quantum dots

2003 J. Phys. A: Math. Gen. 36 5899

(http://iopscience.iop.org/0305-4470/36/22/310)

INSTITUTE OF PHYSICS PUBLISHING JOURNAL OF PHYSICS A: MATHEMATICAL AND GENERAL

J. Phys. A: Math. Gen. **36** (2003) 5899–5904 PII: S0305-4470(03)55105-8

Excitonic clusters in coupled quantum dots

A V Filinov[1,2], **M Bonitz**[1] **and Yu E Lozovik**[2]

[1] FB Physik, Universität Rostock, Universitätsplatz 3, D-18051 Rostock, Germany
[2] Institute of Spectroscopy, RAS, Moscow Region, Troitsk 142190, Russia

Received 22 October 2002, in final form 27 November 2002
Published 22 May 2003
Online at stacks.iop.org/JPhysA/36/5899

Abstract

We present a first-principles path integral Monte Carlo study of a finite number of strongly correlated electron–hole pairs in two symmetric vertically coupled quantum dots. In this system, the intra- and interdot correlations depend on the distance d between the dots, the density n (strength of confinement potential) and temperature T. For fixed d and $T > 0$, increasing n leads to four qualitatively different states: an exciton 'liquid', an exciton 'crystal', orientationally decoupled electron and hole 'crystals' and an electron (hole) liquid.

PACS numbers: 71.35.−y, 73.22.−f, 71.10.−w

1. Introduction

Electron–hole systems have been the subject of extensive experimental and theoretical investigation in the last few decades. In particular, electron–hole symmetric and asymmetric double quantum wells (DQWs) [1] and vertically coupled quantum dots [2] are attracting a lot of interest. In biased DQWs excitons can be photoexcited where electrons and holes are confined in adjacent QWs and, therefore, are spatially separated (interwell (IW) excitons). These excitons are characterized by radiative decay times much longer than those of intrawell excitons, where both carriers are in the same well. Therefore, IW excitons can attain a high density at low temperature T and even Bose condense, as theoretically predicted [3–5]. Alternatively, high IW exciton densities can be achieved by applying an external field in each QW so that electrons and holes are confined in two coupled 2D quantum dots (QDs). The external field may be realized by a system of metallic gates attached to the surface of a semiconductor layer or by self-assembled quantum dots. The distance d between the dots can be made sufficiently large so that interdot tunnelling is negligible. Also, by changing the external field parameters, the exciton density can be varied over a wide range, allowing us to investigate the effects of exciton–exciton correlations[3, 4].

[3] An analysis of classical macroscopic e–h bilayers is performed in [6].
[4] Quantum macroscopic e–h bilayers have been investigated in [7].

The analogous one-component system (consisting only of electrons or holes) in two coupled QWs and QDs has recently been considered theoretically (e.g. [8–11]). In particular, for two coupled dots containing electrons the formation of a mesoscopic cluster has been found and analysed as a function of interdot distance [11]. Furthermore, the increased stability of this mesoscopic cluster compared to a cluster in an isolated QD was revealed at specific interdot separation [8, 11].

In this paper, we report on computer simulations of two symmetric 2D QDs, one containing a small number of electrons, the other the same number of holes. In particular, we are interested in the interplay between Wigner crystallization in the layers and its coexistence with IW excitons. In order to give a reliable answer to these questions, we perform path integral Monte Carlo simulations (PIMC) fully including quantum effects which are crucial for the behaviour of excitons and their correlations.

2. Model and numerical aspects

In the present work we concentrate on a 2D model system which allows us to understand the basic Coulomb correlation effects. More realistic material properties, such as finite layer thickness of the QDs, interdot tunnelling or band anisotropy may become important when the interdot distance is comparable with the exciton Bohr radius a_B and will be considered elsewhere. We use the following Hamiltonian of two vertically coupled electron–hole QDs

$$\begin{aligned} \hat{H} &= H_e + H_h - \sum_{i=1}^{N_e}\sum_{j=1}^{N_h} \frac{e_i e_j}{\epsilon\sqrt{|\mathbf{r}_i - \mathbf{r}_j|^2 + d^2}} \\ \hat{H}_k &= \sum_{i=1}^{N_k}\left[-\frac{\hbar^2}{2m_i}\nabla^2 + V_k(\mathbf{r}_i) + \sum_{i<j}^{N_k}\frac{e_i e_j}{\epsilon|\mathbf{r}_i - \mathbf{r}_j|}\right] \qquad k = e, h \end{aligned} \tag{1}$$

where m_i and e_i are masses and charges of particles (here we consider symmetric bilayers, so $m_e = m_h = m^*$ is the common effective mass of electrons and holes). Further, we take dielectric constants ϵ of the well and surrounding material to be the same. The confinement potential for electrons, V_e, and holes, V_h, is considered as a harmonic potential, $\frac{1}{2}m\omega_i^2 r^2$, with $\omega_e = \omega_h$. In the following, we use the effective Hartree $\mathrm{Ha} = e^2/\epsilon a_B$ as the (atomic) unit of energy and the effective Bohr radius $a_B = \hbar^2\epsilon/m^* e^2$ as the unit of length. Temperature T is also given in atomic units.

To compute the thermodynamic properties of the system of N_e electrons and N_h holes, we evaluate the density operator, $\hat{\rho} = \exp[-\beta\hat{H}]$, where $\beta = 1/k_B T$, which contains complete information about the system and any observable $\hat{O}$,

$$\langle\hat{O}\rangle = \frac{\mathrm{Tr}[\hat{O}\hat{\rho}(\beta)]}{\mathrm{Tr}\,[\hat{\rho}(\beta)]} = \int \mathrm{d}\mathbf{R}\langle\mathbf{R}|\hat{O}\hat{\rho}(\beta)|\mathbf{R}\rangle \Big/ \int \mathrm{d}\mathbf{R}\langle\mathbf{R}|\hat{\rho}(\beta)|\mathbf{R}\rangle \tag{2}$$

where $\mathbf{R} = \{\mathbf{r}_1, \ldots, \mathbf{r}_N\}$ specifies the coordinates of all particles, and $\langle\mathbf{R}|\hat{\rho}(\beta)|\mathbf{R}'\rangle = \rho(\mathbf{R}, \mathbf{R}'; \beta)$ is the N-particle density matrix. While for a correlated system $\hat{\rho}$ is unknown, at high tempatures it can be expanded in terms of one-particle $\rho^{[1]}$, two-particle, $\rho^{[2]}$, etc contributions, and for sufficiently high temperature all terms except the first two can be neglected. As a result, the N-particle density matrix is approximated by

$$\rho(\mathbf{R}, \mathbf{R}'; \tau) \approx \prod_i^N \rho^{[1]}(\mathbf{r}_i, \mathbf{r}_i'; \tau) \prod_{j<k} \frac{\rho^{[2]}(\mathbf{r}_j, \mathbf{r}_k, \mathbf{r}_j', \mathbf{r}_k'; \tau)}{\rho^{[1]}(\mathbf{r}_i, \mathbf{r}_i'; \tau)\rho^{[1]}(\mathbf{r}_k, \mathbf{r}_k'; \tau)} + O(\rho^{[3]}). \tag{3}$$

To take advantage of this high-temperature approximation we use the identity $\hat{\rho}(\beta) = [\hat{\rho}(\tau)]^M$ with $M = \beta/\tau$, where each factor $\hat{\rho}(\tau)$ corresponds to an M times higher temperature, $1/\tau = M \times k_B T$. Choosing M sufficiently large, we can apply the pair approximation (3). We numerically solve the equation for the two-particle density matrix $\rho^{[2]}$ (Bloch equation) using the *matrix squaring technique* [12]. Inserting this result into equation (3) we obtain $\rho(\tau)$. Finally, $\rho(\beta)$ at the required temperature $1/\beta$ follows from the factorization identity by using path integral Monte Carlo techniques (e.g. [13, 10]).

3. Simulation results

We have performed PIMC simulations for a system with $N_e = N_h = 3$ particles per dot and at various values of the interdot distance. The electron and hole densities are controlled by the strength of the confinement which was chosen to be equal in the dots, $V_e = V_h = \frac{1}{2}m\omega^2 r^2$. In the used atomic system of units V[Ha] $= \frac{1}{2}\Omega^2(r/a_B)^2$, where $\Omega = m\omega^2 a_B^3 \epsilon/e^2$. Furthermore, the densities in the layers are influenced by the interlayer correlations, i.e. depend on the distance d. For the sake of comparison with the results for a one-component system in a single QD where the density is controlled by the quantum parameter n, see [10], we use the same parameter which obeys $\Omega = \sqrt{2}n^3$. Below we show results where the quantum parameter was varied in the range $0.05 \leqslant n \leqslant 0.30$ (in a single QD melting of mesoscopic electron clusters was found at $n \sim 0.12$ [10]). The temperature of the system was fixed at 1×10^{-3} Ha assuring that IW excitons are stable. Initially, the system was equlibrated during $\sim 10^4$ MC steps (each step includes movement of all particles). Then all thermodynamical properties were calculated taking the average over $\sim 1.6 \times 10^6$ MC steps.

The simulations are governed by two competing effects—the strong intralayer Coulomb repulsion of particles of the same charge and the interlayer attraction between electrons and holes, where the former may lead to 'crystallization' in the layers and the latter favours the formation of IW excitons. Of special interest is the interplay of these two effects. First, for $d \lesssim 2a_B$, we do not observe 'crystallization' which is due to weakening (screening) of the Coulomb interaction. More interesting behaviour is found at larger d; as an example we present results for $d = 10a_B$. Our results reveal the existence of four different phases[5]: (a) exciton liquid, (b) exciton clusters (mesoscopic exciton crystal), (c) orientationally decoupled clusters (crystals) of electrons and holes and (d) electron–hole liquid. We identify the different phases from an analysis of the intra- and interlayer pair distribution functions (PDF) and the relative interparticle distance fluctuations.

Figure 1 shows the e–h PDF $g_{eh}(r)$ for four densities n. At $n = 0.05$, the first peak of $g_{eh}(r)$ shows that electrons and holes are bound in pairs (excitons), with the effective Bohr radius $a_B^{\text{eff}} \approx 6a_B$ (r denotes the projection of r_{eh} onto one of the layers, i.e. does not include the interdot separation d). The second peak at $r \approx 120a_B$ arises from the next hole in another exciton. Between these two peaks the PDF drops to zero confirming that there is no exchange (tunnelling) of particles between neighbouring excitons. The inset shows the probability density of electrons (upper inset) and holes (lower inset) in their respective QD (one electron—shown by a small cross or square—was fixed and placed at the maximum of the radial distribution function). From the insets one can see that, at $n = 0.05$, the two other excitons are randomly distributed around the fixed electron which allows us to conclude that we observe a state of disordered excitons resembling an exciton 'liquid'. In the next figure

[5] We will use the notions of phases, liquid, crystal etc to underline the analogy to the related phenomena in macroscopic systems.

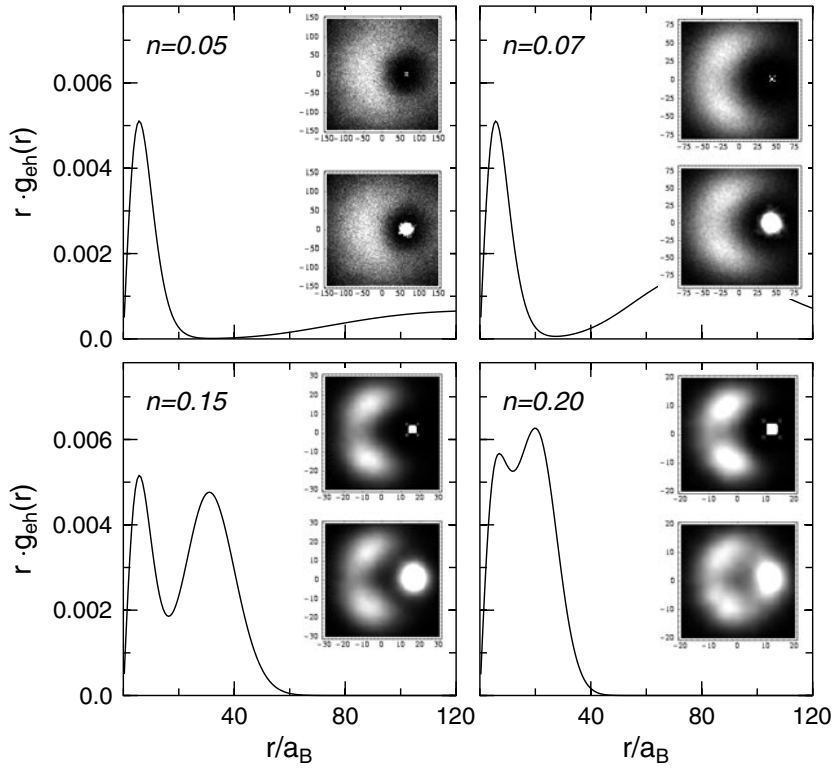

Figure 1. Electron–hole pair distribution function, $r \times g(r)$ (r denotes the projection of r_{eh} on the QW plane) for $N_e = N_h = 3$, for $T = 1/3 \times 10^{-3}$ Ha and $d = 10a_B$ at four values of the confinement: $n = 0.05, 0.07, 0.15$ and 0.20. The insets show the two-dimensional distribution functions in the two layers (one of the electrons—shown by the dot in the upper insets—is fixed).

($n = 0.07$, stronger confinement) we observe a similiar behaviour, only the average distance between the excitons has shrunk to $r \approx 80a_B$.

A qualitatively different picture is observed at $n = 0.15$: here, in each dot all particles are well localized as in a crystal [10] and, at the same time, each electron sits right on top of its hole partner. The inter-exciton correlations are strong enough (at temperature $T = 1/3 \times 10^{-3}$ Ha) to form a radially ordered mesoscopic cluster with all excitons residing on one shell with the same radius, $R_e = R_h \approx 16a_B$. This state is best described as a 'mesoscopic exciton crystal'. Next, at $n = 0.20$ a third configuration is observed where the particles in each of the dots are localized (as seen in the upper inset), but the hole cluster becomes orientationally decoupled with respect to the electrons (as seen in the smeared out positions of the holes in the lower inset). At the same time the e–h PDF shows that the distance between neighbouring excitons is now reduced to $20a_B$ and the two peaks overlap strongly. At these conditions exchange of particles between excitons becomes frequent. This analysis suggests calling this phase 'orientationally disordered crystal' (decoupled electron and hole crystals). Finally, if the density is increased further, we observe quantum melting of the crystal in each dot (not shown in figure 1), and the system goes over into a liquid-like state.

The most sensitive quantities to characterize the structural properties and to locate the structural transitions are the relative distance fluctuations of particle pairs in the same and in different QDs, Δr_{ee} and Δr_{eh}, and also radial fluctuations of each particle with respect

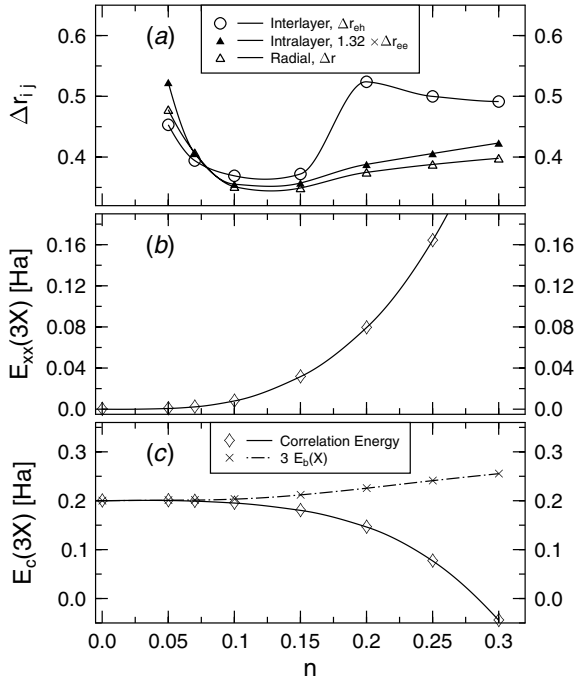

Figure 2. Low-temperature ($T = 1/3 \times 10^{-3}$ Ha) density dependence of: (a) relative radial fluctuations and e–e and e–h distance fluctuations, (b) exciton–exciton interaction energy $E_{xx}(3X)$ of three coupled IW excitons and (c) correlation energy $E_c(3X)$ and binding energy of a single exciton $E_b(X)$.

to the QD centre, Δr, shown in figure 2(a). With the formation of the excitonic cluster at $n \geqslant 0.07$, all fluctuations reach a minimum, while at $n \geqslant 0.15$, fluctuations Δr_{eh} rapidly increase again. Since, at this point, Δr_{ee} and Δr increase only weakly, we conclude that in each dot crystallization persists but the clusters become rotationally decoupled.

Let us now consider the interaction between the IW excitons in more detail (figures 2(b), (c)). To this end, we define the exciton–exciton interaction energy E_{xx}, the correlation energy of the whole system E_c and the binding of a single exciton E_b:

$$E_b(X) = E_e + E_h - E(X) \qquad E_{xx}(3X) = E(3X) - 3E(X) \tag{4}$$

$$E(NX) = NE_e + NE_h + E_c(NX) \tag{5}$$

where $E_{e(h)}$ is the energy of a free electron (hole) in the QD, and $E(X)$, and $E(3X)$ denote the total energy of one and three e–h pairs in the two coupled QDs, respectively. As can be seen from figure 2(b) at $n \leqslant 0.07$ the interaction energy of the three excitons, E_{xx}, is practically zero which is due to the fact that the QD confinement is sufficiently flat and excitons are far apart. When the density exceeds 0.07, E_{xx} increases continuously which reflects a steady increase of the exciton–exciton repulsion until it leads to a break-up of rigid e–h pairs and the possibility of the relative rotation of the electron and hole clusters, cf the density distributions in the insets of figure 1 at $n = 0.20$. Finally, in figure 2(c) we show the density dependence of the binding energy of a single exciton and of the correlation energy $E_c(3X)$. Interestingly, E_b increases with the confinement which is due to the reduction of the quantum extension of electrons (and holes). The correlation energy which can be rewritten

as $E_c(3X) = 3E_b(X) - E_{xx}(3X)$, contains both excitonic and exciton–exciton repulsion effects, decreases with increased confinement because the increase of E_{xx} is the dominant effect.

4. Summary

This work is devoted to the investigation of electron–hole pairs located in two separated quantum dots. We presented an analysis of excitonic states and 'crystallization' in this system. We obtained a finite density interval where the excitons can form mesoscopic clusters. Upon compression these clusters melt via loss of orientational order between the electrons and holes in the two dots. Similarly, as in macroscopic e–h bilayers [9, 6], the electron–hole attraction leads to a stabilization of the mesoscopic clusters compared to the case of a single QD [10] from $r_s \sim 45$ to $r_s \sim 20$.[6] One can make the following estimations of the typical temperatures and densities where e–h clusters in bilayers can be observed ($T \lesssim 1/3 \times 10^{-3}$ Ha, $r_s \gtrsim 20$): for GaAs-based structures, $T \lesssim 40$ mK and $\rho \lesssim 8 \times 10^8\,\mathrm{cm}^{-2}$; for CdTe, $T \lesssim 100$ mK and $\rho \lesssim 9 \times 10^9\,\mathrm{cm}^{-2}$; for ZnSe, $T \lesssim 400$ mK and $\rho \lesssim 3 \times 10^9\,\mathrm{cm}^{-2}$.

Acknowledgments

We thank Dr Donko for making his results on classical e–h bilayers [6] available to us prior to publication. This work has been supported by the Deutsche Forschungsgemeinschaft (BO-1366/2) and by a grant for CPU time at the NIC Jülich.

References

[1] Timofeev V B and Larionov A V *et al* 2000 *Phys. Rev.* B **61** 8420, and references therein
[2] Anisimovas E and Peeters F M 2002 *Phys. Rev.* B **65** 233302
Anisimovas E and Peeters F M 2002 *Phys. Rev.* B **66** 075311
[3] Lozovik Yu E and Yudson V I 1976 *Zh. Eksp. Teor. Fiz.* **71** 738 (Engl. transl. 1976 *Sov. Phys.–JETP* **44** 386)
Lozovik Yu E and Yudson V I 1976 *Solid State Commun.* **19** 391
[4] Lozovik Yu E and Berman O L 1997 *Phys. Scr.* **55** 491
[5] Zhu X and Littlewood P B *et al* 1995 *Phys. Rev. Lett.* **74** 1633
[6] Hartmann P, Donko Z and Kalman G *Phys. Rev. Lett.* submitted
[7] De Palo S, Rapisarda F and Senatore G 2002 *Phys. Rev. Lett.* **88** 206401
[8] Goldoni G and Peeters F M 1996 *Phys. Rev.* B **53** 4591
Schweigert I V, Schweigert V A and Peeters F M 1999 *Phys. Rev. Lett.* **82** 5293
[9] Rapisarda F and Senatore G 1998 *Strongly Coupled Coulomb Systems* ed G Kalman *et al* (New York: Plenum) p 529
[10] Filinov A V, Lozovik Yu E and Bonitz M 2000 *Phys. Stat. Sol.* (b) **221** 231
Bonitz M, Golubnychiy V, Filinov A V and Lozovik Yu E 2002 *Microelectron. Engng.* **63** 141
[11] Filinov A V, Bonitz M and Lozovik Yu E 2001 *Contrib. Plasma Phys.* **41** 357
[12] Storer R G 1968 *J. Math. Phys.* **9** 964
[13] Ceperley D 1995 *Rev. Mod. Phys.* **67** 279

[6] Values of r_s were obtained from the mean interparticle distance which follows from the first maximum of the intralayer pair distribution function. The value $r_s = 20$ roughly corresponds to the orientational melting (decoupling) of the clusters in the two layers.